7

Biological Diagnosis Based on Microfluidics and Nanotechnology

Navid Kashaninejad[1,2], Mohammad Yaghoobi[3], Mohammad Pourhassan-Moghaddam[1,4], Sajad R. Bazaz[1,4], Dayong Jin[2,4], and Majid E. Warkiani[1,4,5]

[1] University of Technology Sydney, School of Biomedical Engineering, Faculty of Engineering and Information Technology, Broadway, Sydney, NSW 2007, Australia
[2] University of Technology Sydney, School of Mathematical and Physical Sciences, Faculty of Science, Broadway, Sydney, NSW 2007, Australia
[3] Sharif University of Technology, Department of Mechanical Engineering, Azadi, Tehran 11155, Iran
[4] University of Technology Sydney, Institute for Biomedical Materials and Devices (IBMD), Faculty of Science, Broadway, Sydney, NSW 2007, Australia
[5] Sechenov University, Institute of Molecular Medicine, Pyrogovskaya, Moscow 119991, Russia

7.1 Introduction

Early diagnosis of diseases is of paramount importance, especially for managing chronic and asymptomatic illnesses. As such, the synergistic effect of combining nanotechnology with microfluidics can significantly improve biological diagnosis. Both organic and nonorganic nanoparticles have been used for clinical imaging and disease diagnosis [1]. Target molecules can interact with these nanoparticles for ultrasensitive detection of some *in vivo* and *in vitro* biological changes. The emergence of microfluidics with the capability of integrating various laboratory processes on a single chip, known as micro total analysis systems (μTAS) or lab-on-a-chip [2–11], has the potential to revolutionize the field of biological diagnosis.

One strategy to diagnose a disease is to use biosensors for the aim of detecting biochemical analytes – small molecules, proteins, cardiac, or cancer biomarkers – in patients' blood, urine, or other biological samples [12]. Numerous techniques can be used to create detectable signals for measuring the concentration or relative quantity of a specific bioanalyte [13]. For this purpose, optical, electrochemical, calorimetric, and piezoelectric transducers have been explored, extensively. Optical biosensors have gained attention in biosensing applications where they are used to study the different properties of targets/analytes and are useful in real-time and parallel detection assays with high precision [14, 15].

Among the numerous types of optical detection techniques, fluorescent nanomaterial-based approaches are broadly used in biological, medical, and drug discovery testing [16]. However, not all fluorescent nanomaterials provide

Nanotechnology and Microfluidics, First Edition. Edited by Xingyu Jiang.

robust, stable, or long-term luminosity. They mostly suffer from photobleaching, low quantum yields (QYs), and narrow emission spectra. The main problems associated with fluorescence methods can be addressed by using semiconductor quantum dots (Qdots) possessing unique optical properties. Their surface is capable of being modified with various biomolecules making them selective to different analytes [17, 18]. They can be then used in bulk solution assays (as colloidal suspension) or solid-phase assays (as immobilized on the surface). Upconversion nanoparticles (UCNPs) are another type of fluorescent nanomaterials that have been used in photoluminescent (PL) detection. UCNPs can be used for bioimaging, biosensing, and drug delivery [19]. The higher excitation wavelength of these nanoparticles adds a multitude of advantages to this type of nanoparticle. The last generation of fluorescent nanomaterials, namely carbon-based Qdots or simply "biodots," has generated interest because of their exceptional properties that are useful in the biomedical imaging [20]. Their properties include high QY, water bioavailability, multicolor wavelength emission, and exceptional biocompatibility. Innovative approaches of nanobiosensing using fluorescent nanomaterials are performed in microfluidic devices. Moreover, because of the movement of flow, the nonspecific deposition of these nanoparticles is reduced, and their reaction rates with targets are increased in microfluidic-based assays because of the nanoscale mixing [21].

Microfluidics is an enabling technology that can be employed in numerous biological studies because of its high-throughput, precision, sample efficiency, portability, and low-cost production [13, 21–26]. Three types of microfluidics used in bioanalysis are continuous, droplet-based, and digital microfluidics (DMFs) [17, 27], each of which has its advantages and disadvantages. Integrated microfluidic devices combined with multiplexed immunoassays provide an opportunity for this technology to facilitate point-of-care (POC) diagnostics [28] for diseases such as cancer [29], malaria [30], or some other abnormalities [31]. Herein, we first describe the functions of Qdots, UCNPs, and biodots; afterward, the applications of nanoparticles-based microfluidics for disease diagnosis will be highlighted. Further, we expand upon the new trends in biological diagnosis platforms by discussing two emerging formats of microfluidics: digital and paper-based microfluidics.

7.2 Quantum Dot-Based Microfluidic Biosensor for Biological Diagnosis

Qdots are nano-sized particles with binary compounds of elements with II–IV, III–V, and IV–VI number of valence electrons and semiconductor materials that present many advantages over fluorescent proteins and organic dyes. Their emission spectra are dependent on their size and excitation wavelength, ranging from ultraviolet to infrared. It is possible to excite multiple Qdots only by single wavelength [32], which makes them suitable for multiplexed detection assays. In other words, Qdots absorption spectra cover a broad span of wavelengths. They have a high QY and long fluorescent lifetime suitable for long-term biological

assays. Photostability and resistance to photobleaching are also other essential characteristics of Qdots [33].

Moreover, they can be used as donors and sometimes as acceptors in energy transfer-based assays because of their unique optical properties. Fluorescence resonance energy transfer (FRET) is a method for measuring distances as small as 1 nm up to 20 nm. In this phenomenon, the nonradiative energy transfer between two fluorescent components (called donor and acceptor) is sensitive to the distance between (d) them where this energy is inversely proportional to the d^6 of this distance. The donor needs to be excited by an external light source, and acceptor's absorption and donor's emission range should have an overlap. Beyond the range of 1–20 nm, no energy transfer occurs [17]. Also, there are several other methods of energy transfer such as chemiluminescence resonance energy transfer (CRET), which have been described in the literature [32]. Qdots can serve as donor or acceptor to improve the efficiency of energy transfer, implementing all aforementioned optical characteristics [34].

Nevertheless, the distance itself is not always the case, especially in biorecognition events. It has been mentioned that if the distance is less than 20 nm, energy transfer will take place. In this range, a fluorescent-labeled bioanalyte is coupled to a biofunctionalized Qdot. Therefore, the bioanalyte is detected with an optical detector. This optical detection is the most common application of Qdots in biosensing.

7.2.1 Qdot-Based Disease Diagnosis Using Microfluidics

In the bioanalysis with Qdots, these nanoparticles are conjugated with biomolecules for the detection of analytes. In the case of a disease, the target analytes can be viruses, antigens, and cancer biomarkers, whose concentration is also of interest. As such, in a study, Hu et al. produced stable antibody-conjugated-Qdots in the aqueous phase and used them in a microfluidic chip for multiplexed detection of carcinoma embryonic antigen (CEA) and α-fetoprotein (AFP) in both sandwich and reversed-phase immunoassays (Figure 7.1) [35], indicating an excellent capability for POC cancer diagnosis.

In addition to small-volume usage of sample and reagent as well as reducing the time-to-result provided by microfluidics, this technology allows for better manipulation of flow in order to enhance the capture efficiency of targets onto the biofunctionalized reaction sites. This opportunity is used by Ng et al. [36] for the detection of QD-labeled SkBr3 (breast cancer) or fluorescein isothiocyanate (FITC)-labeled Colo205 (colon cancer) cells by capturing them onto both nanoporous silica anti-EpCAM (epithelial cell adhesion molecule)-coated substrate and the polydimethylsiloxane (PDMS)-stamped areas of this plate inked with antibody solution (Figure 7.2).

Cancer is not the only field of applicability of the Qdot-based microfluidic assays. Infectious disease can also be detected or monitored using such assays. Klostranec et al. [20] proposed an IgG (goat antimouse)-conjugated Qdot barcode microbead sandwich assay for the detection of HBV (hepatitis B virus), HCV (hepatitis C virus), and human immunodeficiency virus (HIV) antigens. A spiked human serum with corresponding antibodies was incubated with the

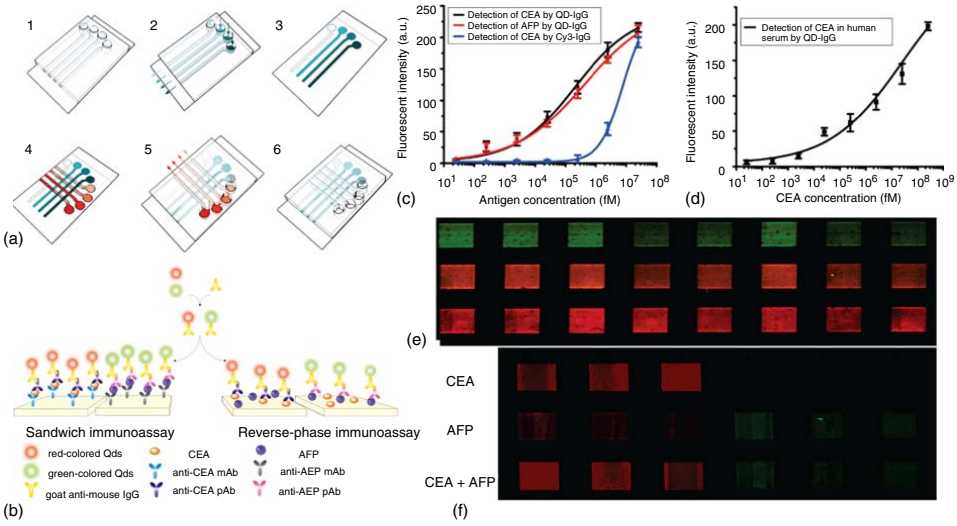

Figure 7.1 (a) Illustration of the process of making a two-dimensional array of immobilized protein layers. (b) Schematic of sandwich and reversed-phase immunoassay with CEA and AFP antibodies and antigens. (c) The dose–response calibration curve for CEA and AFP based on the QD-IgG probes and microfluidic network chip. The measured concentration ranges from 25 fM to 25 nM with limit of detection (LOD) as low as 250 fM (S/N > 3) for both targets. (d) CEA concentration in human serum ranging from 25 fM to 250 nM and LOD was 2.5 pM. The presence of serum albumin slightly hinders antibody–antigen reaction, but still, the tests show better sensitivity in comparison to PBS buffer detection. (e) Three different types of Qdots with green, orange, and red colors excited only under UV illumination for a CEA concentration of 25 pM. (f) The multiplexed ability of Qdots with red and green emission colors. Horizontal channels associate with CEA, AFP, and CEA-AFP mixtures from top to bottom, respectively. The perpendicular microchannels 1-3 are filled with red-colored emitting QD-IgG and 4–6 with green-colored emitting QD-IgG. Source: Hu et al. 2009 [35]. Reproduced with permission of American Chemical Society.

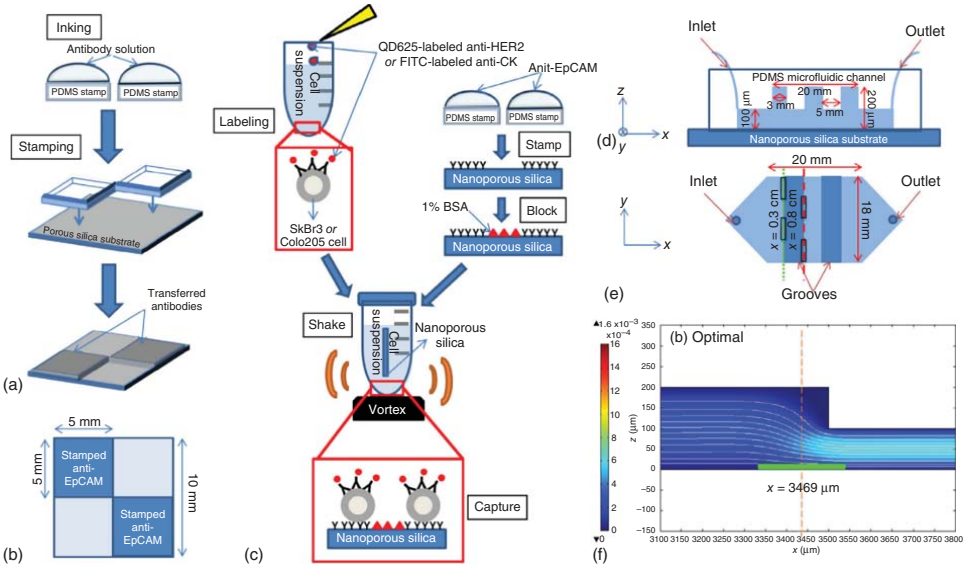

Figure 7.2 (a) Schematic of stamped nanoporous manufacturing process (microcontact printing). (b) Top view of the resulting substrate. (c) Immunofluorescence schematic procedure of detection of cancer cells labeled with Qdots or fluorescent dye. The detection of cells whose nuclei were stained with DAPI was performed by fluorescent microscopy. (d) Side view of the grooved microfluidic device is used to exploit the ability of microfluidics to create optimal sites for labeled cancer cells and (e) top view of the same device. (f) Optimal site for capturing cells are located where the vertical component of velocity is downward and significantly enough to push them toward the reaction area. This area is shown in green color. Source: Ng et al. 2013 [36]. Reproduced with permission of Elsevier.

biofunctionalized Qdots. This assay (Figure 7.3) suggests a fast (less than an hour) diagnosis with 50 times greater sensitivity compared to FDA-approved ELISA (enzyme-linked immunosorbent assay) technique, which has many disadvantages, including high costs and lower multiplexing capability. As the polystyrene Qdot barcode flow through the focused laser point, a detection signal is recorded. Then, this output barcode signal is interpreted. The green signal is associated with the AlexaFluor-488, and the peaks indicate the passage of every single bead, while red, yellow, and their combination specify the type of antigen.

Among infectious diseases, influenza virus detection is of paramount importance because of its severe health complications and the challenges in the virus classifications. Therefore, a wealth of research has been undertaken to address these issues. Zhang et al. [37] proposed a simultaneous detection of H1N1, H3N2, and H9N2, as well as subtyping of them, using integrated micromagnet field microfluidic chip within 80 min interval and LOD of 10–20 nM concentration of the viruses' genetic material. The capture probe DNAs (CP-DNAs) were immobilized on the surface of supermagnetic beads (SMB). These conjugated probes were then injected into the integrated microfluidic device to react with the target cDNAs (T-DNAs or DNAs of influenza A viruses) injected from another side. Each sample was injected through different neighboring channels that made it possible to analyze the genetic samples of all three viruses simultaneously. The assay is composed of a sandwich structure composed of SMB-(CP-DNA), T-DNA, and (RP-DNA)-biotin-(SA-Qdots) serving as the substrate, target, and detector units, respectively. An ITO heating electrode controlled the temperature of the assay in order to keep the reaction time of DNA as low as possible. In this assay, the normalized fluorescent intensities of T-DNAs in 1 μM solutions were optimized under 45 °C, and the DNA hybridization reaction time was 25 minutes. The concentration of H1N1 and H9N2 was a linear function of fluorescent intensity corresponding to 1–150 nM of the target, while H3N2 concentration was linear between 5 and 150 nM of the target (Figure 7.4).

Although there are other studies of influenza, virus detection using Qdots and other microplatforms with more sensitivity and lower LOD [38], low sample usage, and ultrafast manipulation of targets are still exclusive to microfluidics.

Another application of magnetic beads and Qdots (CdSd/CdZnS) was demonstrated by Kim et al. [39] for detection of Plasmodium falciparum histidine-rich protein 2 (pfHRP2), the most common biomarker of malaria, with the aid of microdroplets. The pfHRP2 antibody was conjugated on the surface of Qdots and microbeads (MB). The conjugates were then incubated with human serum containing pfHRP2. After separation of MB-Ab-pfHRP2-Ab-Qdot and elution of Qdots, fluorescence measurements were performed to determine the concentration of HRP2. This process was carried out in an array of six consecutive wells in a PDMS-based microchip (Figure 7.5) and was compared to a standard vial-based assay.

Because of economic reasons, animal health is also monitored through the diagnosis of their diseases, mainly using novel technologies such as microfluidics. For instance, subclinical ketosis (SCK), a disease that affects the cows' products

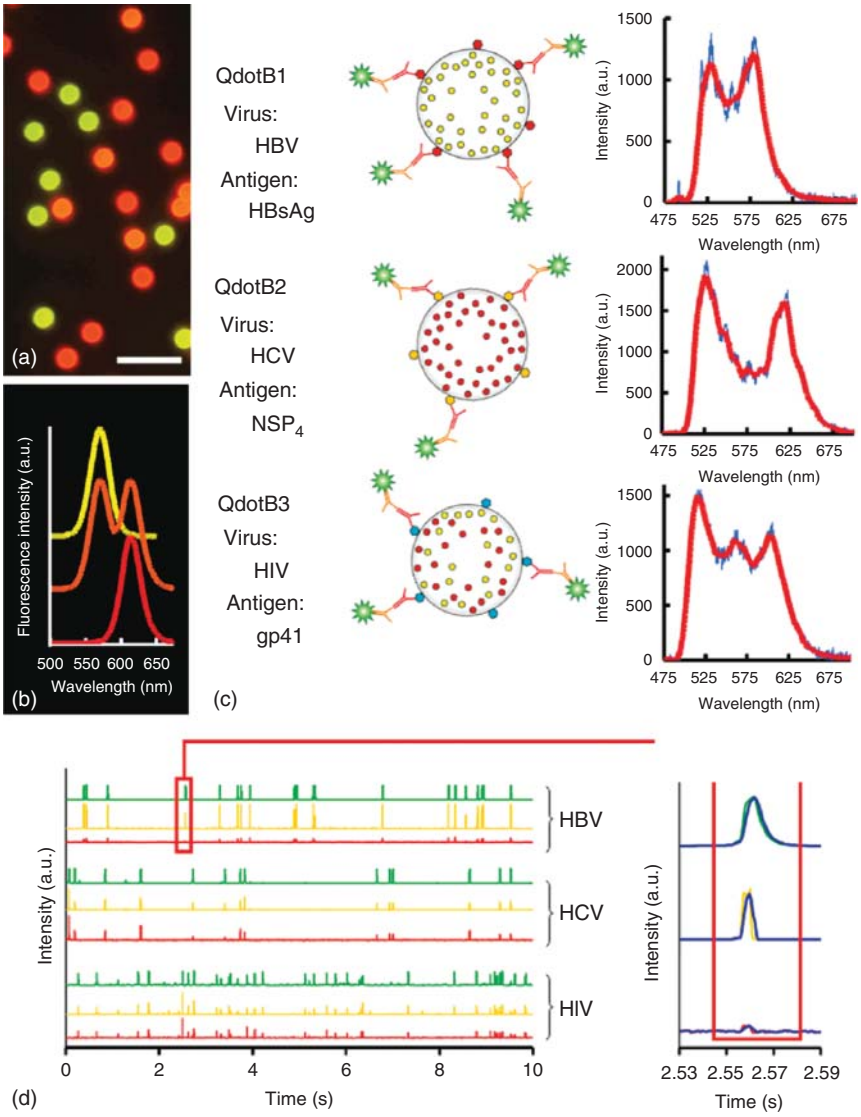

Figure 7.3 (a) A sample of QdotBs with three different emission colors and fluorescent emission spectrums. (b) The orange QdotB is composed of a combination of red and yellow color Qdots, and the bimodal distribution is a sign of that. (c) The three different QdotB microbeads were conjugated with antigens. Antibody-conjugated dye was added to provide a fluorescence detection peak at 520 nm. The other peak in the diagram of intensity–wavelength is related to the corresponding Qdots. (d) An example of the data detected by a photodetector over 10 seconds intervals for green, red, and yellow channels. An HBV antigen-conjugated QdotB crossing the laser spot leads to the peak of green and yellow fluorescent intensity, and red channel signal remains unaffected. Source: Klostranec et al. 2007 [20]. Reproduced with permission of American Chemical Society.

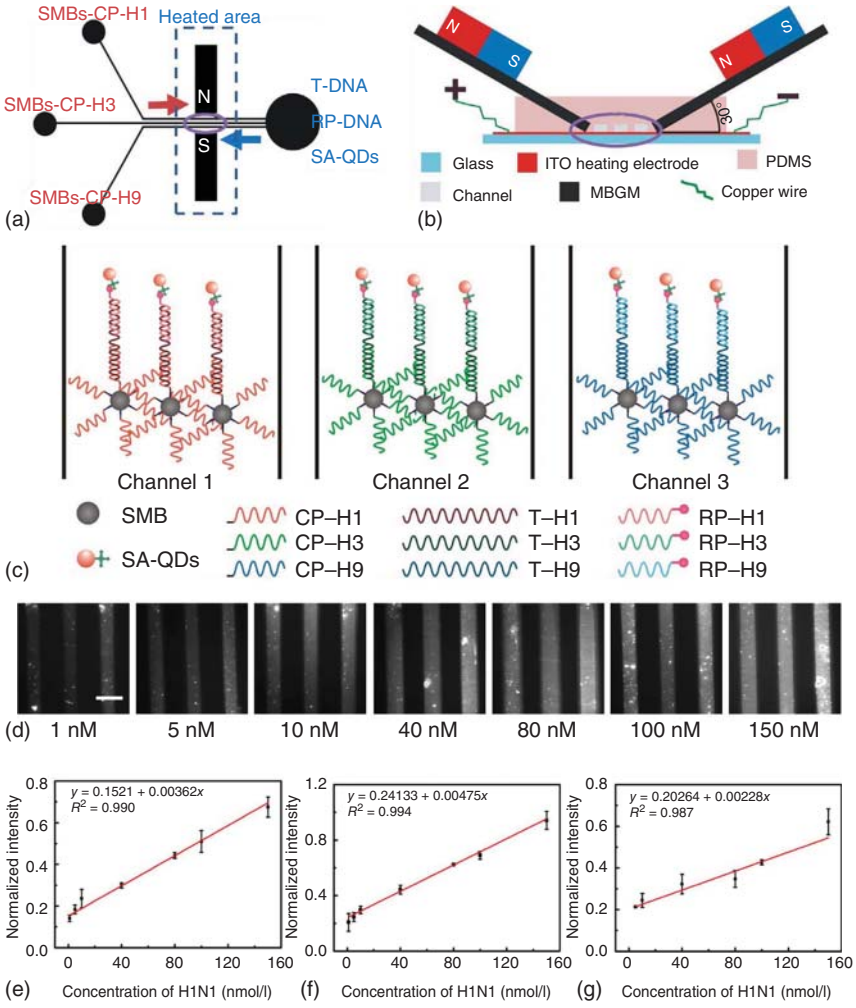

Figure 7.4 (a) Integrated microfluidic schematic diagram and style of different sample loading. (b) Side view of the microfluidic device. (c) Schematic configuration of virus detection and subtyping in the three juxtaposed sandwich assays. (d) The multiplexed detection of the T-DNA solutions and concentration evaluation for different concentrations of H1, H2, and H9 viruses. (e, f) linear dependence of H1 and H9 fluorescent intensity on a concentration within 1–150 nM solutions and (g) linear fluorescent intensity dependence on H2 concentration in 5–150 nM range. Source: Zhang et al. 2018 [37]. Reproduced with permission of Elsevier.

and health, is mainly diagnosed by measuring β-hydroxybutyrate (βHBA) concentration in their blood, urine, or milk. Current diagnostic methods are time-consuming and expensive. On the contrary, a microfluidic device coupled with biofunctionalized Qdots developed by Weng et al. [40] showed sensitive and on-farm detection of SCK. The Qdots were modified with adenine dinucleotide (NAD^+). NAD^+ in the presence of βHBA, as a result of an enzymatic reaction, was converted to NADH that increased the fluorescence intensity of Qdots (Figure 7.6). The serum and pretreated milk samples were tested after 3 min

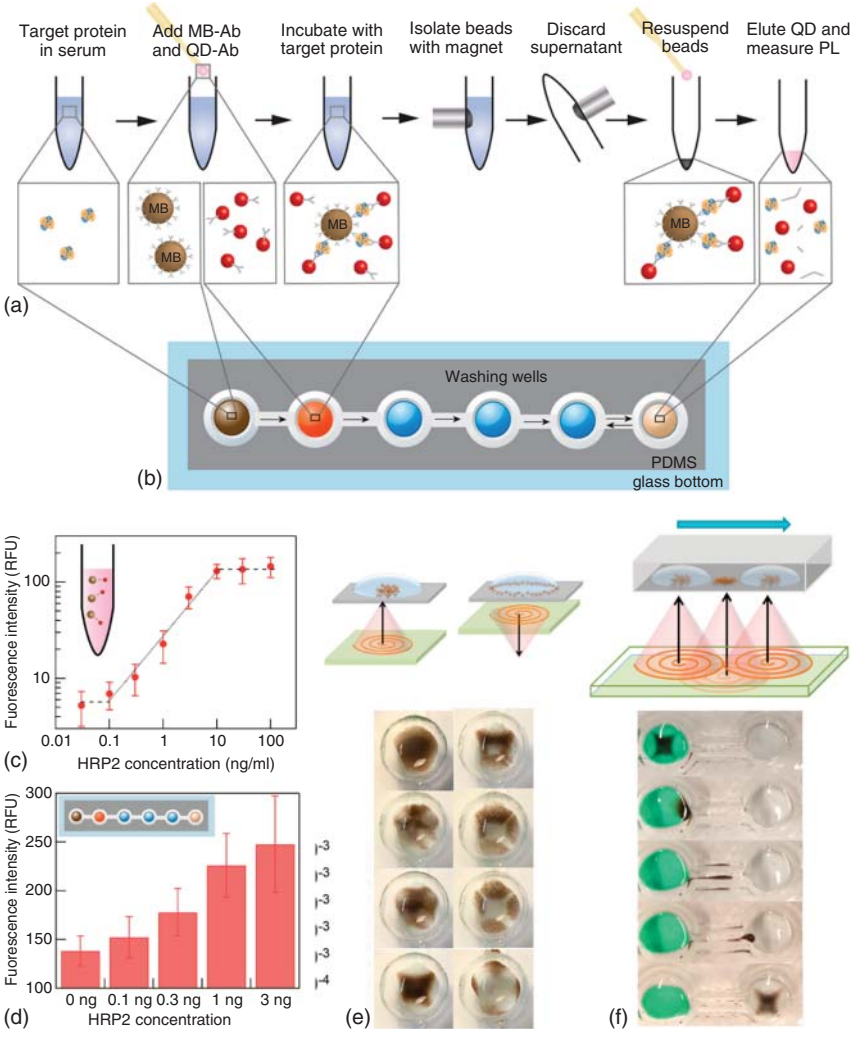

Figure 7.5 (a, b) Schematic illustration of viral-based and microfluidic MB-based assays for detection of pfHRP2 proteins. (c) The vial-based assay results regarding the HRP2 concentration in human serum. The fluorescence intensity and concentration show a linear correlation between 0.1 and 10 ng/ml. (d) The results of MB-based assay show increased RFU for the same concentration of HRP2. (e) Simple agitation/mixing process by changing current direction and (f) translocation of MBs within different wells using PCB. Source: Kim et al. 2017 [39]. Reproduced with permission of American Chemical Society.

of incubation in the microfluidic device. The results of serum-based detection showed a better detection limit compared to those of milk samples.

7.3 Upconversion Nanoparticles

Another type of nanomaterial that has been used in photoluminescence (PL)-based nanobiosensing approached is UCNP. These nanoparticles have to

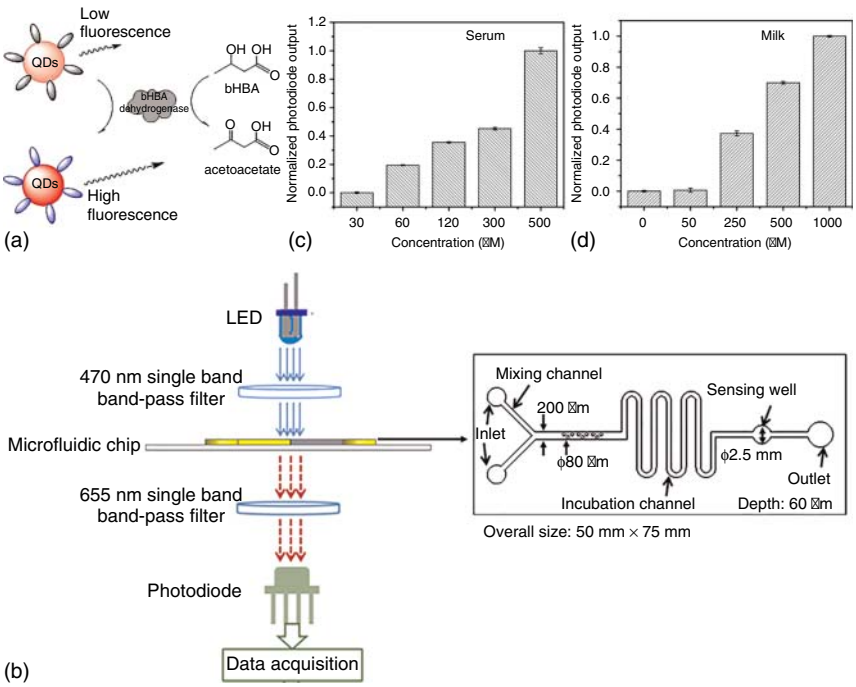

Figure 7.6 (a) Conjugation of NAD+ on the surface of Qdots was performed by immobilization of them on the 3-aminophenylboronic acid monohydrate (APBA)-conjugated Qdots. NAD+ reduces the amount of fluorescent intensity of Qdots through an energy transfer (ET) process. (b) Illustration of microfluidic device and photodiode-equipped platform for diagnosis of SCK. (c) The normalized photodiode intensity versus different concentration of βHBA in serum and (d) milk samples. Source: Weng et al. 2015 [40]. Reproduced with permission of Elsevier.

be excited with a relatively higher wavelength, thus proposing some additional advantages over Qdots or conventional organic dyes. UV is typically used for excitation of PL reagents, which inflict damage on living cells in long-term assays. Moreover, the signal-to-background ratio is usually low in the Qdot- or organic dye-based assays because of scattering of light by living tissues.

Furthermore, Qdots made by heavy metals may have a toxic effect on cells. This can limit their application in biological diagnostics. UCNPs, on the other hand, are excited by near-infrared (NIR) emission in which cells show an optical transparency window. UCNPs also produce a lower level of phototoxicity and light scattering [41]. Similar to Qdots, UCNPs can be coupled with FRET technology, thus improving the sensitivity and selectivity for detection of bioanalytes [42]. UCNPs can also be conjugated with different moieties or antibodies to be prepared for biological assays. In one study, Li et al. [43] were able to detect prostate-specific antigen (PSA) in human serum using luminescence resonance energy transfer (LRET) between UCNPs and gold nanoparticles (GNPs). The UCNP was conjugated with an anti-PSA antibody (donor) to perform a sandwich assay in which the fluorescent emission from the UCNP was quenched after binding with antibody-conjugated GNP (acceptor) (Figure 7.7).

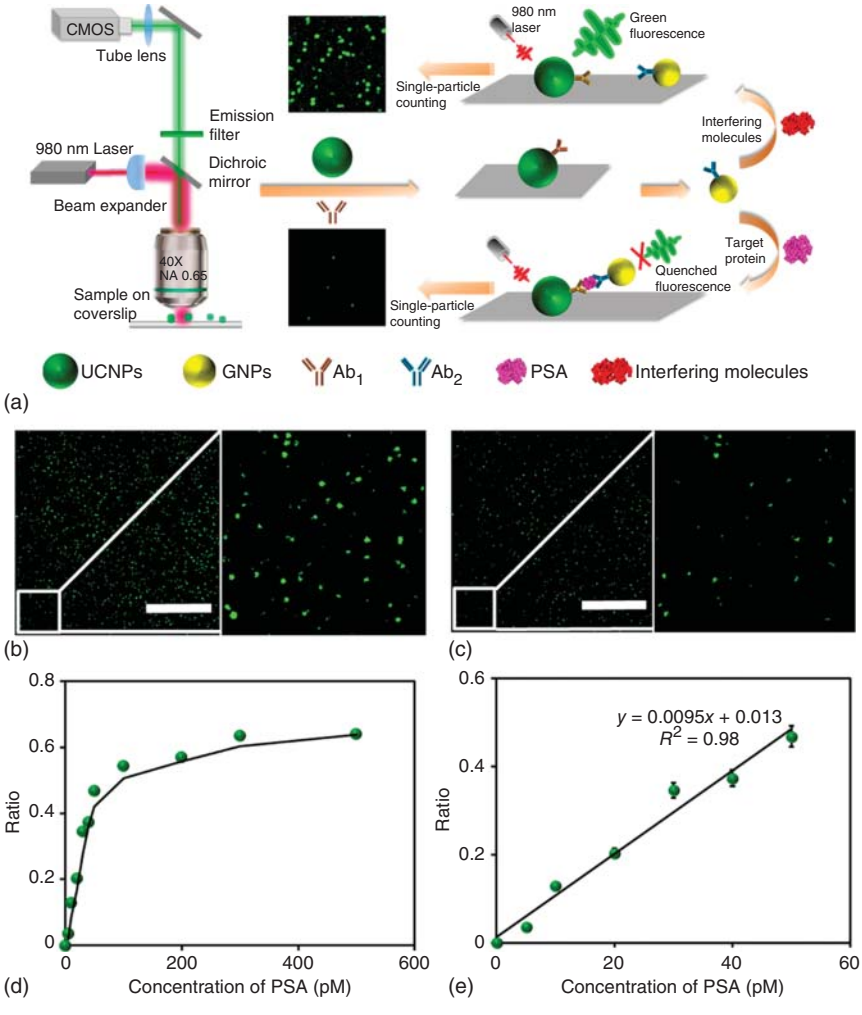

Figure 7.7 (a) Schematic illustration of PSA detection using LRET quenching between UCNPs and GNPs sandwiching specific antigens. The selectivity of the test was examined in the presence of interfering proteins such as IgG and HSA. (b, c) Fluorescence of antibody-conjugated UCNPs on a glass slide and fluorescence quenching after addition of antigen and antibody-conjugated GNPs. (d) The ratio of quenched UCNPs and number of total UCNPs versus the concentration of PSA with LOD of 1.0 pM. The correlation between this ratio and PSA concentration is found to be linear in the range of 0–60 pM concentration of PSA as shown in part (e). Source: Li et al. 2018 [43]. Reproduced with permission of American Chemical Society.

7.4 Fluorescent Biodots

Many investigations are currently underway concerning the imaging of the biological molecules and cellular components using fluorescent nanomaterials. The primary trend is to apply such materials in the precise imaging of the

biological phenomena, which holds promise in the diagnosis and tracking of various biomolecules. The last generation of fluorescent nanomaterials, namely carbon-based Qdots or simply "biodots," has attracted considerable interest because of their exceptional properties that are useful in the biomedical imaging [44]. Their properties, including high QY, water bioavailability, multicolor wavelength emission, and exceptional biocompatibility make them attractive alternatives for the current toxic Qdots. In other words, biodots possess many of the properties of Qdots except for their toxicity, which extends the applicability of these fluorescent nano-sized dots toward *in vivo* environments, including sensing, imaging, drug delivery, and theranostics [45].

Biodots were discovered as a by-product in research work on the preparation of carbon nanotubes [46]. Later, a group dubbed these fluorescent nanostructures as carbon dots (c-dot). The term biodots was later given to carbon dots prepared from biological sources of carbon such as plant extracts [47]. The primary driver for the transition from c-dot to biodots was that many nonbiocompatible compounds were needed to be used in the synthesis of c-dots. Therefore, green approaches were introduced to minimize the environmental risk and to maximize the biocompatibility of c-dots. Therefore, green c-dots are called biodots because of their eco-friendly origin [48]. They are prepared from various natural sources such as plant materials, animal materials, human hair, or biofluids. The source may also include pure biomaterials such as vitamins, carbohydrates, nucleic acids, and proteins [49]. The main feature of biodots is their exceptional optical properties, including high resistance to the photobleaching, high QY, and multicolor excitation emission as an agent for multiplex imaging [49].

From the chemistry point of view, biodots are mainly composed of oxygen, carbon, hydrogen, and nitrogen atoms. Nevertheless, these atoms are organized in such a way that they can absorb light, be excited, and emit the light in a longer wavelength, hence demonstrating fluorescent properties. Regarding the source material for synthesis, biodots show superior properties, as they are synthesized using natural materials that are cheap and rich in multiple chemical groups, which provide enough passivation of the surface not to require any doping modifications [50].

Several approaches have been devised to prepare different types of biodots. These methods are mainly classified into two strategies: "top-down" and "bottom-up" [51, 52]. In top-down approaches, the biodots are created by breaking down the bulk sources such as multiwalled carbon nanotubes or graphite materials under harsh physical or chemical conditions [47, 53, 54]. Whereas in the bottom-up approaches, biodots are synthesized by the association of small organic molecules, which exist in biological materials such as carbohydrates, under various conditions. In most bottom-up methods, heat is recruited as the primary tool for the formation of the fluorescent molecular structures, where hydrothermal heating, microwave pyrolysis, and ultrasonication are among frequently used techniques [55–57]. The most suitable method for preparation of biodots is hydrothermal treatment, which is affordable and straightforward and uses nontoxic material. The source material is converted to biodots through a multistage process including dehydration, polymerization, carbonization, and passivation [58–60] (Figure 7.8).

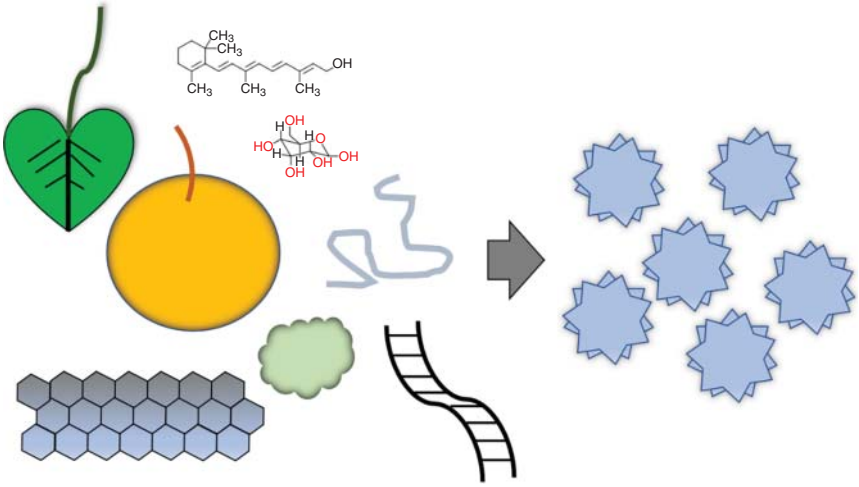

Figure 7.8 Various natural resources for the synthesis of fluorescent biodots. Biodots are synthesized from various carbon sources including nucleic acids, proteins, plant material, graphene, and small molecules. The linear carbon atoms produce rings. The fluorescence properties of biodots originate from the rings that can absorb light and emit it in higher wavelengths.

7.5 Digital Microfluidic Systems for Diagnosis Detection

One of the main aims of microfluidics is to be utilized as an easy-to-use POC system for rapid diagnosis and disease detection [61]. DMFs is one of the growing fields within the microfluidic community with great promise for translation into the practice [62]. Discrete droplets are manipulated within DMF platforms by electrostatic forces. Numerous operations can be carried out for droplets in DMF systems such as mixing, merging, transport, dispensing, and splitting [63]. These systems do not require any pumps or valves and can handle several droplets while specific processes are performed, independently. In addition, these devices do not require any predesigned inlets and outlets, and a specific flow path is not defined for them. These salient features enable scientists to integrate multistep immunoassays into a single microfluidic-based POC device [64].

Generally, DMF systems are categorized into two classes: open and closed systems. In the open classification, droplets are placed on top of a plate where electrodes are installed at the bottom layer of the device, and each of them can be controlled individually. Jain et al. investigated the effect of electrode geometry on the velocity of droplets in an open DMF system. In this study, electrode patterns with the shape of zigzag-flat, zigzag, interdigital, and square were evaluated both numerically and experimentally. They realized that the configuration of the zigzag-flat electrode led to rapid transportation of droplets [65]. Open DMF devices are characterized to have access to each droplet from the top side, facilitating the delivery of droplets to different locations within the device. A closed system is the one where droplets are surrounded between the top and bottom plate. As the top layer exists, friction also exists that reduces the droplet

velocity. Therefore, these devices have a lower droplet velocity compared to open ones [66]. Unlike the open DMF systems, in closed ones, the grounding is always the top layer.

In the beginning, the detection mechanism for DMF immunoassay was mainly optical, where chemiluminescence or fluorescence was used for detection [67]. Miller et al. developed a DMF device that can directly perform heterogenous immunoassay on the surface of the device [68]. As the heterogenous immunoassay was performed on the surface of the device, directly, the need for BSA (for blocking the surface), beads or magnets, and carrier oil for suspending the media and movement of droplets were eliminated. The schematic workflow of the device is illustrated in Figure 7.9a–c.

The detection method was based on the fluorescent signal where FITC-labeled anti-IgG nanoparticles were used as the detector, and a fluorescence plate reader was utilized for measuring the fluorescence. By a combination of magnetic force and DMF, A.H.C. Ng et al. proposed a new platform for particle-based immunoassay that relied upon chemiluminescent detection [69]. In their platform, they eliminated the usage of carrier oil, where the reagent volume, as well as processing time, was reduced to 100 and 10 times, respectively. The mechanism and schematic illustration of the device is shown in Figure 7.1d–f. In another work, Choi et al. proposed an automated DMF platform for magnetic particle-based immunoassays based on chemiluminescent detection [70]. Their automated platform contained a 90 Pogo pin interface for DMF control, an integrated, motorized detector for detection, and a magnetic lens assembly that can facilitate simultaneous (up to eight) DMF magnetic separation. Furthermore, their platform enabled investigators to gain the efficiency of design of experiment protocol for optimization of immunoassay performance.

Recently, a DMF immunoassay was developed based on electrochemical detection [67]. As illustrated in Figure 7.9g, gold sensing and silver counting/pseudoreference electrodes were added to the upper plate. Then, stimulating thyroid hormone (TSH) was captured by the primary antibody (mounted on top of magnetic beads), and the captured TSH was recognized by a horseradish peroxidase enzyme (HRP)-labeled anti-TSH antibody. Afterward, the positive signal was detected through oxidation of 3,3′,5,5′-tetramethylbenzidine by HRP.

Loop-mediated isothermal amplification (LAMP) is an emerging method for diagnosis and detection because it can be operated at a constant temperature while maintaining its high efficiency. Thus, the requirements of reaction facilities are simplified, dramatically. The combination of DMF with LAMP can be considered as the next step toward molecular detection. Wan et al. proposed a DMF–LAMP system for sequence-specific pathogen detection [71]. In their system, they improved their technique in several aspects, including a considerable reduction in reagent consumption, increasing the sensitivity of the technique through a short incubation time, and real-time monitoring. Also, Coelho et al. proposed a specific DMF platform for LAMP-based amplification of *c-Myc* oncogene as a cancer biomarker [72]. Their proposed device had a retrieving reservoir in which reagent transport, LAMP reaction, and product withdrawal occur.

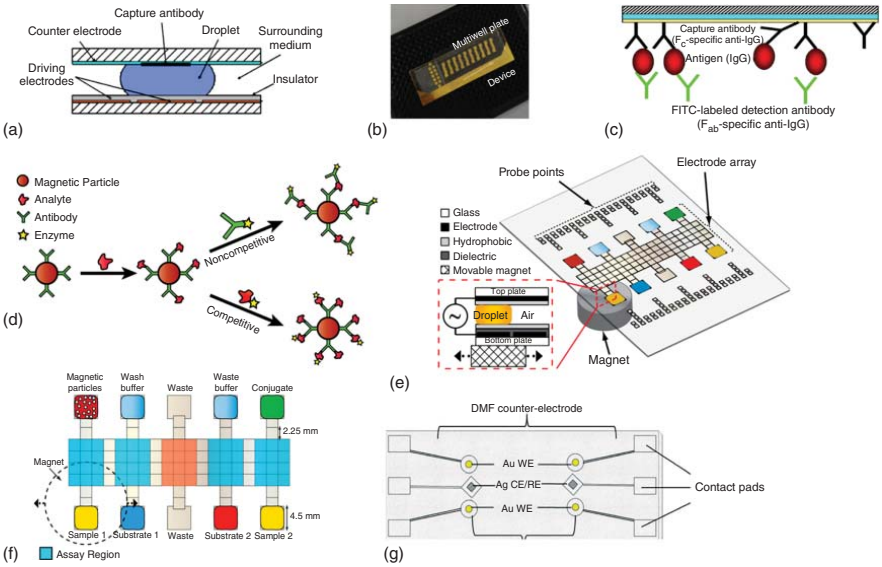

Figure 7.9 Digital microfluidics for biological diagnosis. (a) Driving electrodes lead to movement of droplets. (b) Illustration of the 10-platform device. The DMF device is placed on top of a multiwell plate for the aim of fluorescence detection. (c) Schematic illustration of the detection method. The top plate is first decorated with the captured antibody. Then, binds with IgG that binds FITC-labeled anti-IgG. (d) Schematic depicting of competitive and noncompetitive immunoassay in the presence of magnetic particles. (e) Isometric and (f) top view of the proposed design by Ng et al.. A movable magnet was mounted at the bottom of the device for immobilization of particles. Source: Ng et al. 2012 [69]. Reproduced with permission of American Chemical Society. (g) Schematic illustration of the top plate from top view. The top plate was patterned with indium tin oxide to contain gold sensing and silver counter/pseudo-reference electrodes.

7.6 Paper-Based Diagnostics

7.6.1 Structure and Chemistry of Paper

Paper, a planar thin material, is prepared through processing of wood-based resources such as trees where the cellulose fibers of pulp are squeezed together. Because of the capillary wicking of water in the paper, it is used as a substrate for the fabrication of channels and reservoirs in which fluid can flow. Furthermore, the paper is a cheap material, and microfluidic structures can easily be implemented by using simple desktop printers and heaters. In other words, the main feature of paper-based microfluidic devices is their exceptional potential for mass production [73–75].

Therefore, many methods are being developed to fabricate paper-based microfluidic devices, also known as microfluidic paper-based analytical devices (μPADs). Nevertheless, the core technique is to print the desired pattern, such as channels and reservoirs, from a hydrophobic ink on the paper substrates, followed by curing the printed structure [75, 76].

Different types of papers are used as the device substrate to meet specific requirements. For instance, papers with smaller pore sizes transport the fluid more quickly. The difference in the chemical structure is another factor that affects the selection of paper substrates, where for instance, nitrocellulose paper is used for the detection of biomolecular analytes [77, 78].

As mentioned earlier, paper-based diagnostic devices have more potential than non-paper-based devices for upscaling and commercialization. Nevertheless, some disadvantages may hamper their use for accurate detection of diseases. The main issue is that paper has low mechanical durability, and its porous structure may interfere with a homogenous biorecognition reaction that may result in nonreproducible results. Furthermore, it is not a suitable device for continuous analyses where multiple steps are needed to complete the biorecognition reaction. Another issue with paper-based (bio)-sensing is that paper-based readout signals are not as robust as the standard diagnostic assays. Different strategies are recruited to address some of the above issues. In order to obtain the maximum efficiency, modification of the texture and surface of the paper is undertaken to improve the functionality of the device [79]. For example, in order to increase the speed of the liquid in the device, glutaraldehyde is used for cross-linking the paper texture. This cross-linking produces smaller pores in the paper texture and leads to a more rapid liquid mass transportation [78, 80]. Another strategy for improvement of the physicochemical properties of paper-based devices is to blend them with other materials such as polymeric materials including chitosan and plastic. This blending renders more flexibility and durability to the paper while keeping its desirable physicochemical properties [80, 81].

In order to increase the signal intensity, numerous approaches are being applied, where incorporation of signal amplification steps is the most common strategy. These signal amplification steps can be biological, nanomaterial-based, or a combination of these methods. A typical example of biological signal amplification is the application of enzymes, such as HRP, in the detection

process. The main reason for the application of enzymes is that they transduce a single biorecognition event into a detectable signal through the conversion of several substrate molecules into detectable products [82, 83].

In other strategies, bimolecular targets, such as nucleic acids, are amplified by using *in vitro* nucleic acid amplification methods, where the amount of target nucleic acid is increased to a detectable level [84–86].

Apart from biological entities, nanomaterials, particularly nanoparticles, serve as new platforms of signal amplification. For this purpose, nanomaterials can be used to carry thousands of signal molecules where the recognition event can trigger the release of these signal molecules, which are traceable as detectable readouts [83, 87].

In addition to their signal-carrying capabilities, nanomaterials can serve as artificial enzymes that mimic the function of natural enzymes and can catalyze a signal amplification reaction similar to that of natural enzymes. Furthermore, nanomaterials of metallic origin are widely used as microelectrodes to facilitate the transduction of the electrochemical signals into the readout zone of paper-based devices [88].

In recent strategies, a combination of biological and nanomaterial-based signal amplification methods are used, where the devices can be used for ultrasensitive detection. A nanobiomaterial of QDs and antibody was used to detect the presence of Aflatoxin B1, in which application of QD-antibody conjugates was able to amplify the positive signal 2 orders of magnitude more than GNP–antibody conjugates [89–91].

7.6.2 Applications of Paper-Based Devices in the Diagnostics

Paper holds promise for fabrication of diagnostic devices owing to the cheap source, biocompatibility, easy surface functionalization, and potential for upscaling. Therefore, paper is best suited for application as a substrate for fabrication of POC diagnostic devices. The application of paper-based devices as POC solutions adds values to existing POC devices in several ways. Facile and almost equipment-free mass production of POC devices is the main contribution of paper-based substrates in the diagnostics industry, which results in the production of very cheap diagnostic kits. In other words, these characteristics facilitate dissemination of these diagnostic devices into remote and underdeveloped areas, which in turn leads to the minimization of disease burden in such locations through affordable diagnosis [76, 92–94].

The most challenging step in the production of paper-based POC diagnostic devices is the integration of *in vitro* diagnostic approaches, such as biosensing methods, into such devices. Based on the readout signal, mainly optical and electrical biosensing methods are integrated into paper-based POC diagnostic devices. Optical biosensing is rather frequent owing to its simplicity, ease of integration, and compatibility with multiplex readouts. Nevertheless, electrical readouts are shown to be more sensitive and can be used in reagent-free detection systems [90, 95–100].

Paper-based biosensing is classified into labeled and label-free categories:

7.6.2.1 Labeled Biosensing

A label is a moiety that functions as a signal molecule while a biorecognition event occurs. The main reason for using a label molecule is that neither detection target nor the detection ligand produces a signal during their interaction. Therefore, a variety of label molecules is conjugated to the ligand, target, or both. Because of the incorporation of labels in the detection process, labeled biosensing tends to give a more sensitive signal. However, as the sensing counterparts (target and ligand) need to be modified, labeling may negatively affect the activity of the target and the ligand.

Furthermore, the labeling contributes to a higher fabrication cost. Depending on the chemical properties of the sensing counterparts and the required accuracy, a variety of label molecules is applied. Optical label molecules are the most commonly used moieties, which are detected visually or by using a reader instrument such as UV–Vis spectrophotometer or fluorescence reading machine. The optical labels range from small chemical molecules to biomacromolecules, where a variety of chemistries are applied to acquire the biorecognition signal [101].

7.6.2.2 Label-Free Biosensing

In label-free biosensing, no label is used to produce the signal. Instead, the signal is produced through changes in the physicochemical properties of either sensor surface, receptor, ligand, or a combination of these elements. For instance, the recognition event may lead to changes in light reflection, electron transfer, heat transfer, etc. [101, 102].

In paper-based microfluidic devices, the paper matrix is used to deposit the sensing materials including nanomaterials, to produce a target-responsive matrix. For example, for performing electrochemical analysis, conductive materials are deposited as electrodes on the paper substrate where the signal transduction takes place. Lei et al. has deposited a layer of carbon nanotubes, as nanoelectrodes, on a paper device to perform a sensitive electrochemical label-free immunoassay of biotin and streptavidin interaction with a detection limit of 25 ng/ml [103].

The main advantage of label-free methods is their simplicity, where there is no need for labeling. Moreover, the fabrication cost of the device is affordable, and more importantly, the labeling does not destroy the biosensing structure.

7.6.3 Integration of Nanoparticles with Paper-Based Microfluidic Devices

With regard to the exceptional properties of nanomaterials, they are widely integrated into paper-based devices. In this section, we overview the application of a variety of nanomaterials and their roles in these devices.

7.6.3.1 Gold Nanomaterials

Gold nanomaterials are mainly used in paper-based device detection. These nanomaterials possess various exceptional optical properties that originate from the oscillation or resonance of their surface plasmon (SPR). Because the surface plasmon is sensitive to the refractive index change of the surrounding

media, it is used to design various plasmonic-based nanobiosensors. When an object, regardless of its origin, binds to the surface of gold nanomaterials, the surface plasmon is changed, which gives rise to a change in the optical signal. The mentioned object can be neighboring nanoparticles or direct deposition of chemical layers on gold nanomaterials. In its most simple configuration, the change in SPR can lead to a color change that can be applied for the visual detection of targets in paper-based devices. In this context, the aggregation and seed-mediated growth of GNPs are used to detect the analyte. Aggregation of GNPs induces a color change; similarly, the seed-mediated growth leads to the amplification of specifically surface-bound GNPs that serve as nuclei of the gold nanomaterials deposition [104].

As an example of gold nanomaterial-based visual detection, GNPs were used to detect the presence of tuberculosis bacterium (TB) DNA. The study showed that TB DNA could induce aggregation of GNPs, which leads to a change in color in the GNP solution, and the intensity of this color change can be analyzed after transferring the complete reaction to wax-printed microwells on paper. Later, the image of each reaction zone is captured by a mobile phone and then analyzed to quantify the extent of signal intensity. In this work, the paper serves as an adsorbent to remove the fluid of the reaction (Figure 7.10a) [105].

In addition to infectious disease biosensing, GNP-based signal amplification was recruited to detect cancer protein biomarkers. In this detection method, authors report on the application of a gold nanobioconjugate that carries multiple HRP signal molecules and the recognition antibody. In this work, a nitrocellulose paper substrate was used to blot the sample, followed by the addition of the as-prepared nanobioconjugate. In the next step, detection is performed based on the HRP–TMB reaction. Compared to conventional ELISA, this method was shown to lead to more intense color development, indicating the signal amplification of the nanobioconjugate (Figure 7.10b) [83].

In addition to optical detection chemistries, gold nanomaterial-based electrodes have been integrated into paper-based devices to improve the limit of the detection figure of merits. In some configurations, the electrode was printed on the paper substrate using screen-printing technology, and microfluidic structures were fabricated using photolithography. This device has been used to detect several bioanalytes using oxidase enzyme reactions, in which the electrode was used to transfer the produced electrons to signal processing parts [107].

7.6.3.2 Fluorescent Nanomaterials

The high sensitivity of fluorescent nanotags has led to the design of ultrasensitive, yet simple paper-based devices that are used to detect minute quantities of analytes. Nevertheless, in the readout of the nanobiosensing process, a device is needed that can excite and read the fluorescence signals. This issue, however, has been partially addressed by analysis of the signals by using smartphone-based fluorescence detectors.

Qdots [108] and UCNPS [109] are the main classes of the nanomaterials that have been embedded into paper-based devices. As explained in Section 7.2, Qdots are tiny semicrystal fluorescent nanoparticles. These nanoparticles have

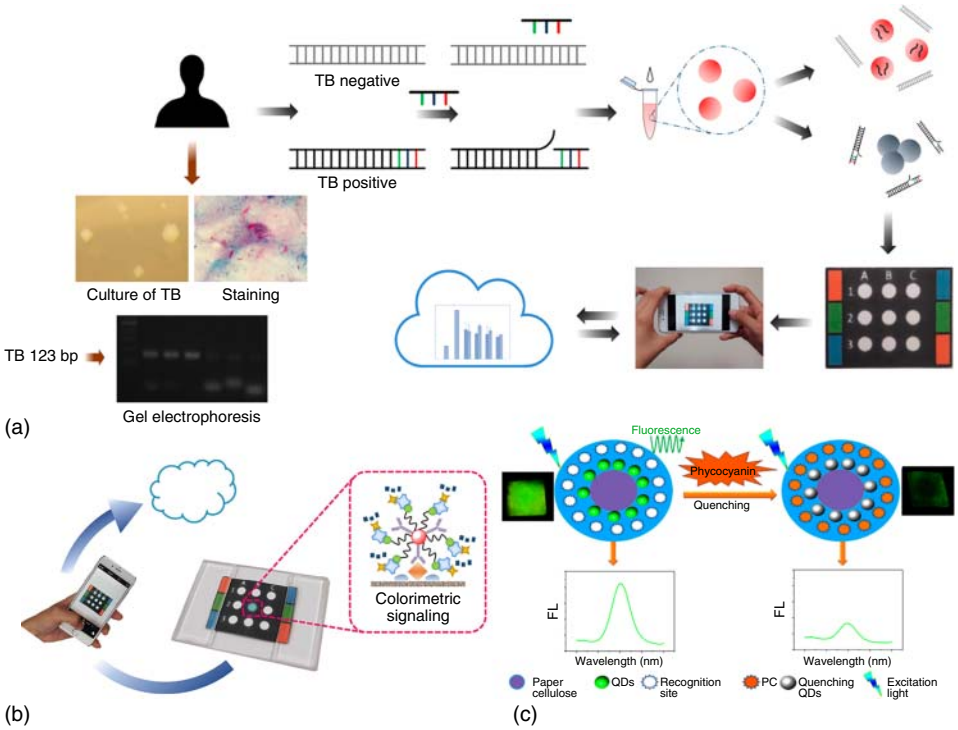

Figure 7.10 Integration of nanoparticles with paper-based microfluidic devices for biological diagnosis. (a) The visual paper-based detection of TB DNA based on the aggregation of gold nanoparticles. Source: Tsai et al. 2017 [105]. Reproduced with permission of American Chemical Society. (b) The paper-based signal amplification for the detection of cancer biomarker. Source: Huang et al. 2018 [83]. Reproduced with permission of American Chemical Society. (c) The principle of the 3D paper device integrated with Qdots for phycocyanin detection. Source: Li et al. 2017 [106]. Reproduced with permission of American Chemical Society.

been used in a variety of paper-based biosensing configurations. In one configuration, an origami-based 3D paper device was used to detect phycocyanin using molecularly imprinted Qdots. When the phycocyanin migrates toward the Qdots and binds to them, the emission of the Qdot is quenched compared with the unbound Qdots, leading to an "on-off" paper-based device (Figure 7.10c) [106].

As discussed in Section 7.3, UCNPs are another class of the fluorescent nanomaterials which have found many applications in ultrasensitive cellular and molecular tracking systems. Therefore, they have been applied to detect targets in paper-based devices because of their exceptionally high QY and prolonged decay. In a study by He et al., a portable UCNP-based paper device has been designed to detect cocaine, where an aptamer-based fluorescence-quenching detection system was applied. In this detection system, GNPs, which had been preconjugated to the free ends of the cocaine aptamer and UCNPs, were immobilized on the paper surface. In its unbound form, the GNP was not located in the vicinity of the UCNP. However, binding of the cocaine to the

aptamer induced the conformational change of the aptamer, which culminated its two ends. This culmination led to quenching of the UCNP signal by the GNP. Therefore, with increases in the concentration of cocaine, the fluorescence decreased in the microwells of the paper-based device [110].

7.7 Conclusion and Future Perspective

Early biological diagnosis means detecting a marker or markers that manifest a particular disease before clinical symptoms. Early detection is crucial for managing chronic diseases such as cancer before further complications. Thus, an efficient diagnostic assay should possess high sensitivity, high selectivity, reliable limit-of-detection, and other analytical metrics. The combination of microfluidics and nanotechnology can lead to the development of highly efficient platforms for effective biological diagnosis. Microfluidics can hugely affect this field by high-throughput production and screening of nanoparticle-based diagnosis, making nanotechnology more appealing for clinical applications. Qdots, UCNPs, and biodots are three principal nanoparticles that are used for biosensing and POC applications. In this chapter, we discussed the integrations of these nanoparticles with microfluidic platforms for biological diagnosis. Furthermore, we evaluated the applications of two emerging formats of microfluidics, i.e. DMFs and paper-based microfluidics, for biological diagnosis.

The application of signal quantification methods, such as image-processing procedures, can be adopted as an efficient strategy to cope with the challenges in signal quantification, which are generated in the microfluidic devices. Currently, the integration of nanomaterials and mobile-based image processing technologies in microfluidic-based diagnostics have opened up a tremendous opportunity for end user scale implementation of analytically robust and fully automated low-cost devices. The less-developed part of microfluidic-based biosensors is the absolute quantification of signals, broadening the dynamic range and the multiplicity of the devices. It is evident that addressing the above challenges requires further efforts in the development of novel readout devices that can analyze the signals in reliable levels and be comparable to standard analytical instruments.

Conflicts of Interest

The authors declare no conflicts of interest.

Acknowledgment

This research work is supported by the National Health and Medical Research Council via the career development fellowship (APP1143377) and the Australian Research Council through discovery project grants (DP170103704 and DP180103003).

References

1 Chen, H., Zhen, Z., Todd, T. et al. (2013). Nanoparticles for improving cancer diagnosis. *Mater. Sci. Eng., R* 74 (3): 35–69.

2 Nguyen, N.-T., Shaegh, S.A.M., Kashaninejad, N., and Phan, D.-T. (2013). Design, fabrication and characterization of drug delivery systems based on lab-on-a-chip technology. *Adv. Drug Deliv. Rev.* 65 (11): 1403–1419.

3 Nguyen, N.-T., Hejazian, M., Ooi, H.C., and Kashaninejad, N. (2017). Recent advances and future perspectives on microfluidic liquid handling. *Micromachines* 8 (6): 186–205.

4 Kashaninejad, N., Nikmaneshi, R.M., Moghadas, H. et al. (2016). Organ-tumor-on-a-chip for chemosensitivity assay: a critical review. *Micromachines* 7 (8): 130–153.

5 Moshksayan, K., Kashaninejad, N., Warkiani, M.E. et al. (2018). Spheroids-on-a-chip: recent advances and design considerations in microfluidic platforms for spheroid formation and culture. *Sens. Actuators, B* 263: 151–176.

6 Kashaninejad, N., Shiddiky, M.J.A., and Nguyen, N.-T. (2018). Advances in microfluidics-based assisted reproductive technology: from sperm sorter to reproductive system-on-a-chip. *Adv. Biosyst.* 2 (3): 1700197.

7 Dinh, T., Phan, H.-P., Kashaninejad, N. et al. (2018). An on-chip SiC MEMS device with integrated heating, sensing, and microfluidic cooling systems. *Adv. Mater. Interfaces* 5 (20): 1800764.

8 Mollajan, M., Bazaz, S.R., and Mehrizi, A.A. (2018). A thoroughgoing design of a rapid-cycle microfluidic droplet-based PCR device to amplify rare DNA strands. *J. Appl. Fluid Mech.* 11 (1): 21–29.

9 Moghadas, H., Saidi, M.S., Kashaninejad, N., and Nguyen, N.-T. (2018). A high-performance polydimethylsiloxane electrospun membrane for cell culture in lab-on-a-chip. *Biomicrofluidics* 12 (2): 024117.

10 Kashaninejad, N., Chan, W.K., and Nguyen, N.-T. (2011). Fluid mechanics of flow through rectangular hydrophobic microchannels, (44632), pp. 647–655.

11 Moghadas, H., Saidi, M.S., Kashaninejad, N., and Nguyen, N.-T. (2018). Challenge in particle delivery to cells in a microfluidic device. *Drug Deliv. Transl. Res.* 8 (3): 830–842.

12 Vashist, S.K., Luppa, P.B., Yeo, L.Y. et al. (2015). Emerging technologies for next-generation point-of-care testing. *Trends Biotechnol.* 33 (11): 692–705.

13 Luka, G., Ahmadi, A., Najjaran, H. et al. (2015). Microfluidics integrated biosensors: a leading technology towards lab-on-a-chip and sensing applications. *Sensors* 15 (12): 30011–30031.

14 Perumal, V. and Hashim, U. (2014). Advances in biosensors: principle, architecture and applications. *J. Appl. Biomed.* 12 (1): 1–15.

15 Tereshchenko, A., Bechelany, M., Viter, R. et al. (2016). Optical biosensors based on ZnO nanostructures: advantages and perspectives. A review. *Sens. Actuators, B* 229: 664–677.

16 Strianese, M., Staiano, M., Ruggiero, G. et al. (2012). Fluorescence-based biosensors. In: *Spectroscopic Methods of Analysis*, Methods in Molecular Biology, vol. 875 (ed. W. Bujalowski), 193–216. Springer.

17 Vannoy, C.H., Tavares, A.J., Noor, M.O. et al. (2011). Biosensing with quantum dots: a microfluidic approach. *Sensors* 11 (10): 9732–9763.

18 Li, Z., Wang, Y., Wang, J. et al. (2010). Rapid and sensitive detection of protein biomarker using a portable fluorescence biosensor based on quantum dots and a lateral flow test strip. *Anal. Chem.* 82 (16): 7008–7014.

19 Tan, G.-R., Wang, M., Hsu, C.-Y. et al. (2016). Small upconverting fluorescent nanoparticles for biosensing and bioimaging. *Adv. Opt. Mater.* 4 (7): 984–997.

20 Klostranec, J.M., Xiang, Q., Farcas, G.A. et al. (2007). Convergence of quantum dot barcodes with microfluidics and signal processing for multiplexed high-throughput infectious disease diagnostics. *Nano Lett.* 7 (9): 2812–2818.

21 Moghadas, H., Saidi, M.S., Kashaninejad, N. et al. (2017). Fabrication and characterization of low-cost, bead-free, durable and hydrophobic electrospun membrane for 3D cell culture. *Biomed. Microdevices* 19 (4): 74.

22 Ghafar-Zadeh, E. (2015). Wireless integrated biosensors for point-of-care diagnostic applications. *Sensors* 15 (2): 3236–3261.

23 Kashaninejad, N., Chan, W.K., and Nguyen, N.-T. (2012). Eccentricity effect of micropatterned surface on contact angle. *Langmuir* 28 (10): 4793–4799.

24 Kashaninejad, N., Nguyen, N.-T., and Chan, W.K. (2012). Eccentricity effects of microhole arrays on drag reduction efficiency of microchannels with a hydrophobic wall. *Phys. Fluids* 24 (11): 112004–112021.

25 Barisam, M., Saidi, S.M., Kashaninejad, N., and Nguyen, N.-T. (2018). Prediction of necrotic core and hypoxic zone of multicellular spheroids in a microbioreactor with a U-shaped barrier. *Micromachines* 9 (3): 94–112.

26 Bazaz, S.R., Mehrizi, A.A., Ghorbani, S. et al. (2018). A hybrid micromixer with planar mixing units. *RSC Adv.* 8 (58): 33103–33120.

27 Lashkaripour, A., Mehrizi, A.A., Goharimanesh, M. et al. (2018). Size-controlled droplet generation in a microfluidic device for rare dna amplification by optimizing its effective parameters. *J. Mech. Med. Biol.* 18 (1): 1850002.

28 Luppa, P.B., Bietenbeck, A., Beaudoin, C., and Giannetti, A. (2016). Clinically relevant analytical techniques, organizational concepts for application and future perspectives of point-of-care testing. *Biotechnol. Adv.* 34 (3): 139–160.

29 Tothill, I.E. (2009). Biosensors for cancer markers diagnosis. *Semin. Cell Dev. Biol.* 20 (1): 55–62

30 Ragavan, K., Kumar, S., Swaraj, S., and Neethirajan, S. (2018). Advances in biosensors and optical assays for diagnosis and detection of malaria. *Biosens. Bioelectron.* 105: 188–210.

31 Lee, W.G., Kim, Y.-G., and Chung, B.G. (2010). Nano/microfluidics for diagnosis of infectious diseases in developing countries. *Adv. Drug Deliv. Rev.* 62 (4–5): 449–457.

32 Zhou, J., Yang, Y., and Zhang, C.-Y. (2015). Toward biocompatible semiconductor quantum dots: from biosynthesis and bioconjugation to biomedical application. *Chem. Rev.* 115 (21): 11669–11717.

33 Petryayeva, E., Algar, W.R., and Medintz, I.L. (2013). Quantum dots in bioanalysis: a review of applications across various platforms for fluorescence spectroscopy and imaging. *Appl. Spectrosc.* 67 (3): 215–252.

34 Chou, K. and Dennis, A. (2015). Förster resonance energy transfer between quantum dot donors and quantum dot acceptors. *Sensors* 15 (6): 13288–13325.

35 Hu, M., Yan, J., He, Y. et al. (2009). Ultrasensitive, multiplexed detection of cancer biomarkers directly in serum by using a quantum dot-based microfluidic protein chip. *ACS Nano* 4 (1): 488–494.

36 Ng, E., Hoshino, K., and Zhang, X. (2013). Microfluidic immunodetection of cancer cells via site-specific microcontact printing of antibodies on nanoporous surface. *Methods* 63 (3): 266–275.

37 Zhang, R.-Q., Hong, S.-L., Wen, C.-Y. et al. (2018). Rapid detection and subtyping of multiple influenza viruses on a microfluidic chip integrated with controllable micro-magnetic field. *Biosens. Bioelectron.* 100: 348–354.

38 Lee, N., Wang, C., and Park, J. (2018). User-friendly point-of-care detection of influenza A (H1N1) virus using light guide in three-dimensional photonic crystal. *RSC Adv.* 8 (41): 22991–22997.

39 Kim, C., Hoffmann, G., and Searson, P.C. (2017). Integrated magnetic bead–quantum dot immunoassay for malaria detection. *ACS Sensors* 2 (6): 766–772.

40 Weng, X., Chen, L., Neethirajan, S., and Duffield, T. (2015). Development of quantum dots-based biosensor towards on-farm detection of subclinical ketosis. *Biosens. Bioelectron.* 72: 140–147.

41 Chen, G., Qiu, H., Prasad, P.N., and Chen, X. (2014). Upconversion nanoparticles: design, nanochemistry, and applications in theranostics. *Chem. Rev.* 114 (10): 5161–5214.

42 Wang, L., Yan, R., Huo, Z. et al. (2005). Fluorescence resonant energy transfer biosensor based on upconversion-luminescent nanoparticles. *Angew. Chem. Int. Ed.* 44 (37): 6054–6057.

43 Li, X., Wei, L., Pan, L. et al. (2018). Homogeneous immunosorbent assay based on single-particle enumeration using upconversion nanoparticles for the sensitive detection of cancer biomarkers. *Anal. Chem.* 90 (7): 4807–4814.

44 Lim, S.Y., Shen, W., and Gao, Z. (2015). Carbon quantum dots and their applications. *Chem. Soc. Rev.* 44 (1): 362–381.

45 Peng, Z., Han, X., Li, S. et al. (2017). Carbon dots: Biomacromolecule interaction, bioimaging and nanomedicine. *Coord. Chem. Rev.* 343: 256–277.

46 Xu, X., Ray, R., Gu, Y. et al. (2004). Electrophoretic analysis and purification of fluorescent single-walled carbon nanotube fragments. *J. Am. Chem. Soc.* 126 (40): 12736–12737.

47 Sun, Y.-P., Zhou, B., Lin, Y. et al. (2006). Quantum-sized carbon dots for bright and colorful photoluminescence. *J. Am. Chem. Soc.* 128 (24): 7756–7757.

48 Shi, L., Li, Y., Li, X. et al. (2015). Facile and eco-friendly synthesis of green fluorescent carbon nanodots for applications in bioimaging, patterning and staining. *Nanoscale* 7 (16): 7394–7401.

49 Baker, S.N. and Baker, G.A. (2010). Luminescent carbon nanodots: emergent nanolights. *Angew. Chem. Int. Ed.* 49 (38): 6726–6744.

50 Sharma, V., Tiwari, P., and Mobin, S.M. (2017). Sustainable carbon-dots: recent advances in green carbon dots for sensing and bioimaging. *J. Mater. Chem. B* 5 (45): 8904–8924.

51 Yang, Z., Li, Z., Xu, M. et al. (2013). Controllable synthesis of fluorescent carbon dots and their detection application as nanoprobes. *Nano-Micro Lett.* 5 (4): 247–259.

52 Miao, P., Han, K., Tang, Y. et al. (2015). Recent advances in carbon nanodots: synthesis, properties and biomedical applications. *Nanoscale* 7 (5): 1586–1595.

53 Zhou, J., Booker, C., Li, R. et al. (2007). An electrochemical avenue to blue luminescent nanocrystals from multiwalled carbon nanotubes (MWCNTs). *J. Am. Chem. Soc.* 129 (4): 744–745.

54 Zheng, X.T., Ananthanarayanan, A., Luo, K.Q., and Chen, P. (2015). Glowing graphene quantum dots and carbon dots: properties, syntheses, and biological applications. *Small* 11 (14): 1620–1636.

55 Li, H., He, X., Liu, Y. et al. (2011). One-step ultrasonic synthesis of water-soluble carbon nanoparticles with excellent photoluminescent properties. *Carbon* 49 (2): 605–609.

56 Wang, C., Xu, Z., Cheng, H. et al. (2015). A hydrothermal route to water-stable luminescent carbon dots as nanosensors for pH and temperature. *Carbon* 82: 87–95.

57 Choi, Y., Thongsai, N., Chae, A. et al. (2017). Microwave-assisted synthesis of luminescent and biocompatible lysine-based carbon quantum dots. *J. Ind. Eng. Chem.* 47: 329–335.

58 Yuan, M., Zhong, R., Gao, H. et al. (2015). One-step, green, and economic synthesis of water-soluble photoluminescent carbon dots by hydrothermal treatment of wheat straw, and their bio-applications in labeling, imaging, and sensing. *Appl. Surf. Sci.* 355: 1136–1144.

59 Liu, Y., Zhao, Y., and Zhang, Y. (2014). One-step green synthesized fluorescent carbon nanodots from bamboo leaves for copper(II) ion detection. *Sens. Actuators, B* 196: 647–652.

60 Roy, P., Chen, P.-C., Periasamy, A.P. et al. (2015). Photoluminescent carbon nanodots: synthesis, physicochemical properties and analytical applications. *Mater. Today* 18 (8): 447–458.

61 Srinivasan, V., Pamula, V.K., and Fair, R.B. (2004). Droplet-based microfluidic lab-on-a-chip for glucose detection. *Anal. Chim. Acta* 507 (1): 145–150.

62 Srinivasan, V., Pamula, V.K., and Fair, R.B. (2004). An integrated digital microfluidic lab-on-a-chip for clinical diagnostics on human physiological fluids. *Lab Chip* 4 (4): 310–315.

63 Yafia, M., Emran, B.J., and Najjaran, H. (2018). Digital microfluidic systems: fundamentals, configurations, techniques, and applications. In: *Microfluidics: Fundamentals, Devices, and Applications* (eds. Y. Song, D. Cheng and L. Zhao), 175–209. Wiley.

64 Sun, J., Xianyu, Y., and Jiang, X. (2014). Point-of-care biochemical assays using gold nanoparticle-implemented microfluidics. *Chem. Soc. Rev.* 43 (17): 6239–6253.
65 Jain, V., Devarasetty, V., and Patrikar, R. (2017). Effect of electrode geometry on droplet velocity in open EWOD based device for digital microfluidics applications. *J. Electrostat.* 87: 11–18.
66 Banerjee, A.N., Qian, S., and Joo, S.W. (2011). High-speed droplet actuation on single-plate electrode arrays. *J. Colloid Interface Sci.* 362 (2): 567–574.
67 Shamsi, M.H., Choi, K., Ng, A.H., and Wheeler, A.R. (2014). A digital microfluidic electrochemical immunoassay. *Lab Chip* 14 (3): 547–554.
68 Miller, E.M., Ng, A.H., Uddayasankar, U., and Wheeler, A.R. (2011). A digital microfluidic approach to heterogeneous immunoassays. *Anal. Bioanal.Chem.* 399 (1): 337–345.
69 Ng, A.H.C., Choi, K., Luoma, R.P. et al. (2012). Digital microfluidic magnetic separation for particle-based immunoassays. *Anal. Chem.* 84 (20): 8805–8812.
70 Choi, K., Ng, A.H., Fobel, R. et al. (2013). Automated digital microfluidic platform for magnetic-particle-based immunoassays with optimization by design of experiments. *Anal. Chem.* 85 (20): 9638–9646.
71 Wan, L., Chen, T., Gao, J. et al. (2017). A digital microfluidic system for loop-mediated isothermal amplification and sequence specific pathogen detection. *Sci. Rep.* 7 (1): 14586.
72 Coelho, B.J., Veigas, B., Águas, H. et al. (2017). A digital microfluidics platform for loop-mediated isothermal amplification detection. *Sensors* 17 (11): 2616.
73 Martinez, A.W., Phillips, S.T., Wiley, B.J. et al. (2008). FLASH: a rapid method for prototyping paper-based microfluidic devices. *Lab Chip* 8 (12): 2146–2150.
74 Faustino, V., Catarino, S.O., Lima, R., and Minas, G. (2016). Biomedical microfluidic devices by using low-cost fabrication techniques: a review. *J. Biomech.* 49 (11): 2280–2292.
75 Akyazi, T., Basabe-Desmonts, L., and Benito-Lopez, F. (2018). Review on microfluidic paper-based analytical devices towards commercialisation. *Anal. Chim. Acta* 1001: 1–17.
76 Yamada, K., Henares, T.G., Suzuki, K., and Citterio, D. (2015). Paper-based inkjet-printed microfluidic analytical devices. *Angew. Chem.* 54 (18): 5294–5310.
77 Hosseini, S., Vázquez-Villegas, P., and Martínez-Chapa, S.O. (2017). Paper and fiber-based bio-diagnostic platforms: current challenges and future needs. *Appl. Sci.* 7 (8): 863–885.
78 Sher, M., Zhuang, R., Demirci, U., and Asghar, W. (2017). Paper-based analytical devices for clinical diagnosis: recent advances in the fabrication techniques and sensing mechanisms. *Expert Rev. Mol. Diagn.* 17 (4): 351–366.
79 Credou, J., Faddoul, R., and Berthelot, T. (2014). One-step and eco-friendly modification of cellulose membranes by polymer grafting. *RSC Adv.* 4 (105): 60959–60969.

80 Wu, T., Du, Y., Yan, N., and Farnood, R. (2015). Cellulose fiber networks reinforced with glutaraldehyde–chitosan complexes. *J. Appl. Polym. Sci.* 132 (33): 42375–42383.

81 Morsy, F.A. and El-Sherbiny, S. (2004). Mechanical properties of coated paper: influence of coating properties and pigment Blends. *J. Mater. Sci.* 39 (24): 7327–7332.

82 Murdock, R.C., Shen, L., Griffin, D.K. et al. (2013). Optimization of a paper-based ELISA for a human performance biomarker. *Anal. Chem.* 85 (23): 11634–11642.

83 Huang, J.Y., Lin, H.-T., Chen, T.-H. et al. (2018). Signal amplified gold nanoparticles for cancer diagnosis on paper-based analytical devices. *ACS Sensors* 3 (1): 174–182.

84 Seok, Y., Joung, H.A., Byun, J.Y. et al. (2017). A paper-based device for performing loop-mediated isothermal amplification with real-time simultaneous detection of multiple DNA targets. *Theranostics* 7 (8): 2220–2230.

85 Altundemir, S., Uguz, A.K., and Ulgen, K. (2017). A review on wax printed microfluidic paper-based devices for international health. *Biomicrofluidics* 11 (4): 041501.

86 Jauset-Rubio, M., Svobodova, M., Mairal, T. et al. (2016). Ultrasensitive, rapid and inexpensive detection of DNA using paper based lateral flow assay. *Sci. Rep.* 6: 37732.

87 Ge, L., Yu, J., Ge, S., and Yan, M. (2014). Lab-on-paper-based devices using chemiluminescence and electrogenerated chemiluminescence detection. *Anal. Bioanal.Chem.* 406 (23): 5613–5630.

88 Han, K.N., Choi, J.-S., and Kwon, J. (2017). Gold nanozyme-based paper chip for colorimetric detection of mercury ions. *Sci. Rep.* 7 (1): 2806.

89 Ren, M., Xu, H., Huang, X. et al. (2014). Immunochromatographic assay for ultrasensitive detection of aflatoxin B(1) in maize by highly luminescent quantum dot beads. *ACS Appl. Mater. Interfaces* 6 (16): 14215–14222.

90 Silveira, C.M., Monteiro, T., and Almeida, M.G. (2016). Biosensing with paper-based miniaturized printed electrodes-A modern trend. *Biosensors (Basel)* 6 (4): 51–67.

91 Ruecha, N., Yamada, K., Suzuki, K., and Citterio, D. (2017). (Bio)Chemical sensors based on paper. In: *Materials for Chemical Sensing* (eds. T.R.L. Cesar Paixão and S.M. Reddy), 29–74. Cham: Springer International Publishing.

92 Tenda, K., van Gerven, B., Arts, R. et al. (2018). Paper-based antibody detection devices using bioluminescent BRET-switching sensor proteins. *Angew. Chem.* 57 (47): 15369–15373.

93 Hamedpour, V., Leardi, R., Suzuki, K., and Citterio, D. (2018). Fabrication of paper-based analytical devices optimized by central composite design. *Analyst* 143 (9): 2102–2108.

94 Yamada, K., Shibata, H., Suzuki, K., and Citterio, D. (2017). Toward practical application of paper-based microfluidics for medical diagnostics: state-of-the-art and challenges. *Lab Chip* 17 (7): 1206–1249.

95 Alhogail, S., Suaifan, G.A.R.Y., and Zourob, M. (2017). Development of rapid and low-cost paper based sensing platform for bacterial detection. *Procedia Technol.* 27: 146–148.

96 Liu, B., Du, D., Hua, X. et al. (2014). Paper-based electrochemical biosensors: from test strips to paper-based microfluidics. *Electroanalysis* 26 (6): 1214–1223.

97 Sin, M.L.Y., Mach, K.E., Wong, P.K., and Liao, J.C. (2014). Advances and challenges in biosensor-based diagnosis of infectious diseases. *Expert Rev. Mol. Diagn.* 14 (2): 225–244.

98 Ulep, T.-H. and Yoon, J.-Y. (2018). Challenges in paper-based fluorogenic optical sensing with smartphones. *Nano Converg.* 5 (1): 14.

99 Shafiee, H., Asghar, W., Inci, F. et al. (2015). Paper and flexible substrates as materials for biosensing platforms to detect multiple biotargets. *Sci. Rep.* 5: 8719.

100 Yang, Y., Noviana, E., Nguyen, M.P. et al. (2017). Paper-based microfluidic devices: emerging themes and applications. *Anal. Chem.* 89 (1): 71–91.

101 Sang, S., Wang, Y., Feng, Q. et al. (2016). Progress of new label-free techniques for biosensors: a review. *Crit. Rev. Biotechnol.* 36 (3): 465–481.

102 Zanchetta, G., Lanfranco, R., Giavazzi, F. et al. (2017). Emerging applications of label-free optical biosensors. *Nanophotonics* 6 (4): 627–645.

103 Lei, K.F., Yang, S.I., Tsai, S.W., and Hsu, H.T. (2015). Paper-based microfluidic sensing device for label-free immunoassay demonstrated by biotin-avidin binding interaction. *Talanta* 134: 264–270.

104 Zhou, W., Gao, X., Liu, D., and Chen, X. (2015). Gold nanoparticles for *in vitro* diagnostics. *Chem. Rev.* 115 (19): 10575–10636.

105 Tsai, T.-T., Huang, C.-Y., Chen, C.-A. et al. (2017). Diagnosis of tuberculosis using colorimetric gold nanoparticles on a paper-based analytical device. *ACS Sensors* 2 (9): 1345–1354.

106 Li, B., Zhang, Z., Qi, J. et al. (2017). Quantum dot-based molecularly imprinted polymers on three-dimensional origami paper microfluidic chip for fluorescence detection of phycocyanin. *ACS Sensors* 2 (2): 243–250.

107 Dungchai, W., Chailapakul, O., and Henry, C.S. (2009). Electrochemical detection for paper-based microfluidics. *Anal. Chem.* 81 (14): 5821–5826.

108 Xu, Y., Wang, X., Zhang, W.L. et al. (2018). Recent progress in two-dimensional inorganic quantum dots. *Chem. Soc. Rev.* 47 (2): 586–625.

109 Wen, S., Zhou, J., Zheng, K. et al. (2018). Advances in highly doped upconversion nanoparticles. *Nat. Commun.* 9 (1): 2415.

110 He, M., Li, Z., Ge, Y., and Liu, Z. (2016). Portable upconversion nanoparticles-based paper device for field testing of drug abuse. *Anal. Chem.* 88 (3): 1530–1534.